Influence of sintering conditions on the electrical properties and the PTCR effect of the multilayer Ba1.005(Ti1−xNbx)O3 ceramics with Ni internal electrode

ARTICLE *in* JOURNAL OF MATERIALS SCIENCE MATERIALS IN ELECTRONICS · DECEMBER 2012

Impact Factor: 1.57 · DOI: 10.1007/s10854-012-0753-2

J Mater Sci: Mater Electron (2012) 23:2202–2209
DOI 10.1007/s10854-012-0753-2

Influence of sintering conditions on the electrical properties and the PTCR effect of the multilayer $Ba_{1.005}(Ti_{1-x}Nb_x)O_3$ ceramics with Ni internal electrode

Xuxin Cheng · Dongxiang Zhou · Qiuyun Fu · Shuping Gong · Dongchen Zhao

Received: 23 March 2012 / Accepted: 7 May 2012 / Published online: 12 June 2012

Abstract The effects of the Nb-dopant content and the sintering conditions on the electrical properties and the positive temperature coefficient of resistance (PTCR) effect of $Ba_{1.005}(Ti_{1-x}Nb_x)O_3$ (BTN) ceramics were investigated, which were sintered at 1,070–1,220 °C for 0.5–6 h in a reducing atmosphere and then re-oxidized at 600–750 °C for 1 h. The results indicated that both the sintering temperature and sintering time affected the electrical properties and the PTCR effect of the multilayer BTN samples, whose room-temperature (RT) resistance first reduced and then increased as a function of the donor–doped concentration at all sintering temperature; moreover, the higher the sintering temperature was, the lower the critical dopant concentration. The BTN ceramics showed a remarkable PTCR effect, with a resistance jump greater by 3.3 orders of magnitude, along with a low RT resistance of 0.3 Ω at a low reoxidated temperature of 600 °C after sintering in a reducing atmosphere.

1 Introduction

Barium titanate ($BaTiO_3$) is a ferroelectric material, which transforms from a tetragonal perovskite structure into a cubic structure [1]. If the ions at the B or A site of $BaTiO_3$ are substituted by small quantities of pentavalent impurities or a trivalent donor, $BaTiO_3$ becomes a semiconducting material and exhibits a significant increase in resistance near the Curie temperature [2, 3]. The phenomenon is well known as the positive temperature coefficient of resistance (PTCR) effect. The best explanation for this effect has been proposed by Heywang [4] and later modified by Jonker [5].

Donor-doped $BaTiO_3$ ceramics exhibit much higher RT resistance and jump ratios when they are fired in air than when fired in a reducing atmosphere; however, low RT resistance of PTCR samples has been prepared by a reduction–reoxidation method [6–8]. In recent years, there has arisen demand for a semiconducting material employed in an overcurrent-protecting element for electrical circuits; the tape casting of semiconducting $BaTiO_3$ has been studied for its potential use in multilayer chip type ceramics [9–11] to further decrease the resistance. Meanwhile, in order to prevent the Ni internal electrodes, the green bodies are co-sintered in a reducing atmosphere. It is important to study the sintering conditions in a reducing atmosphere. Recently, Chung et al. [12] have suggested that the RT resistance is affected by the sintering temperature. Jonker et al. [13] claim that small pentavalent ions occupy titanium sites and are mainly compensated by titanium vacancies. When sintered in a reducing atmosphere, charge compensation is achieved by electrons and titanium vacancies [14]. Brzozowski et al. [15] have confirmed semiconducting $BaTiO_3$ samples with small amounts of Nb_2O_5 lead to high potential barriers; moreover, he has analyzed the compositions of the secondary phases are $Ba_6Ti_{14}Nb_2O_{39}$[16], and proposed that high amount of titanium vacancies could lead to grain growth inhibition [17]. The mobility of titanium vacancies of the ceramics is interpreted to be the major controlling gas/solid diffusion kinetics [18]. Previous studies have focused only on compensating defect mode in Nb-doped barium titanate in air. However, little attention has been paid to the effects of the Nb-dopant content and the sintering conditions on

X. Cheng · D. Zhou · Q. Fu (✉) · S. Gong · D. Zhao
Department of Electronic Science and Technology, Engineering Research Center for Functional Ceramics MOE, Huazhong University of Science and Technology, Luoyu Road 1037, Hongshan District, Wuhan 430074, Hubei, People's Republic of China
e-mail: fuqy@mail.hust.edu.cn

the PTCR characteristics and the electrical properties of the multilayer BTN ceramics with Ni internal electrode in a reducing atmosphere. Therefore, the objective of this study is to investigate the effects of the sintering conditions on the electrical properties and the PTCR characteristics of the multilayer BTN ceramics with Ni internal electrode prepared in a reducing atmosphere.

2 Experimental procedures

The starting materials were high-purity $BaCO_3$ (>99.8 %), TiO_2 (>99.8 %), SiO_2 (>99.99 %), and Nb_2O_5 (>99.99 %), and they were weighed according to the following formula: $Ba_{1.005}(Ti_{1-x}Nb_x)O_3 + 0.05$ mol% SiO_2. In this experiment, the components were mixed by high energy ball milling for 90 min (2,400 r/min) in deionized water using zirconia balls and then calcined at 1,150 °C for 2 h in air. After drying and sieving, the calcined powder was grinded again by wet ball milling for 5 h in a polyurethane jar. After mixing, the dried powder was mixed with dispersant, defoamer, solvent, and binder by ball milling for 18 h in a nylon pot and cast into green sheets of 55-μm thickness by the doctor-blade method. These sheets were laminated at 50 °C to form a ceramic block, which was applied to Ni inner electrodes, and then cut into rectangular blocks (3.6 mm × 1.8 mm × 1.4 mm) (Scheme 1). Subsequently, the binder was removed by heating at 330 °C in air. Sintering was conducted in an aluminum tube at 1,070–1,220 °C for 0.5–6 h in a reducing atmosphere (3 % H_2/N_2), with the heating and cooling rates being 3.33 °C/min. The bulk densities of the sintered specimens were measured using the Archimedes method. The sintered BTN ceramics were re-oxidized at 600–750 °C in air for 1 h, and the surfaces were rubbed with In–Ga alloy (60:40) to form electrodes. Resistance at room temperature was measured by a digital multimeter, and the temperature dependence of resistance was measured in a temperature-programmable furnace (ZWX-B, Huazhong University of Science and Technology, China) at a heating rate of 1.6 °C/min in the range of 25–250 °C. The surface microstructure of the as-fired ceramics was observed using scanning electron microscopy (SEM; TESCAN VEGA 3 EasyProbe, Czech); energy-dispersive X-ray spectrometry (EDS) was used to obtain the morphology and chemical composition of some individual spots of the samples. The average grain size of the BTN ceramics was estimated by the line-intersection method. The phase formation of the as-sintered ceramics was identified at room temperature using an X-ray diffraction (XRD) technique, using CuKα radiation (X'Pert PRO, Philips, the Netherlands). Complex impedance spectroscopy over the range of 100 Hz–35 MHz was measured using an impedance analyzer (HP4294A, Agilent, USA).

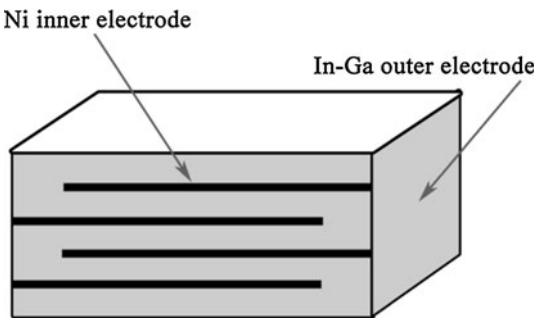

Scheme 1 Schematic cross-sectional view of the multilayer sample with two couple of Ni electrodes

3 Results and discussion

3.1 XRD analysis

Figure 1 shows the XRD patterns of the 0.35 mol% Nb^{5+}–doped BTN ceramics produced by firing at 1,070–1,220 °C for 2 h in a reducing atmosphere, the ceramics sintered at 1,070 °C show a pseudo-monoclinic structure whose

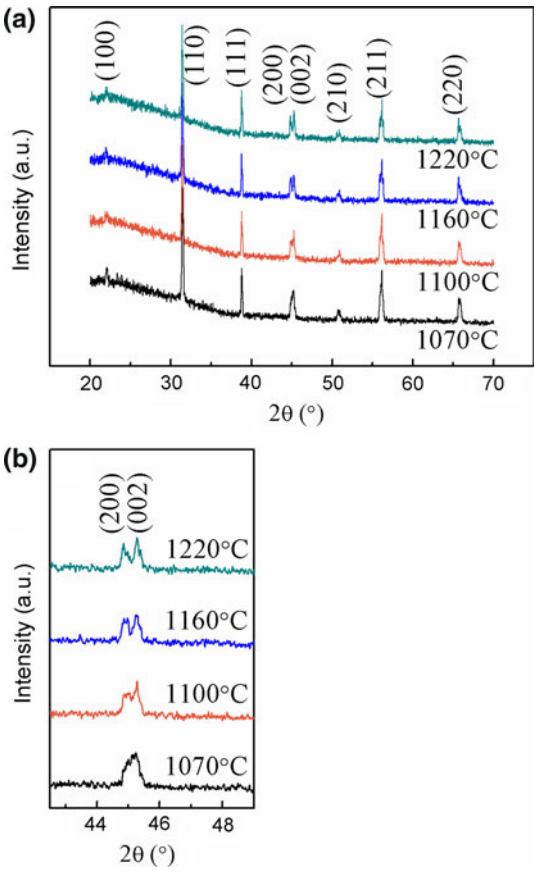

Fig. 1 XRD patterns of the as-sintered BTN specimens sintered at various sintering temperature for 2 h

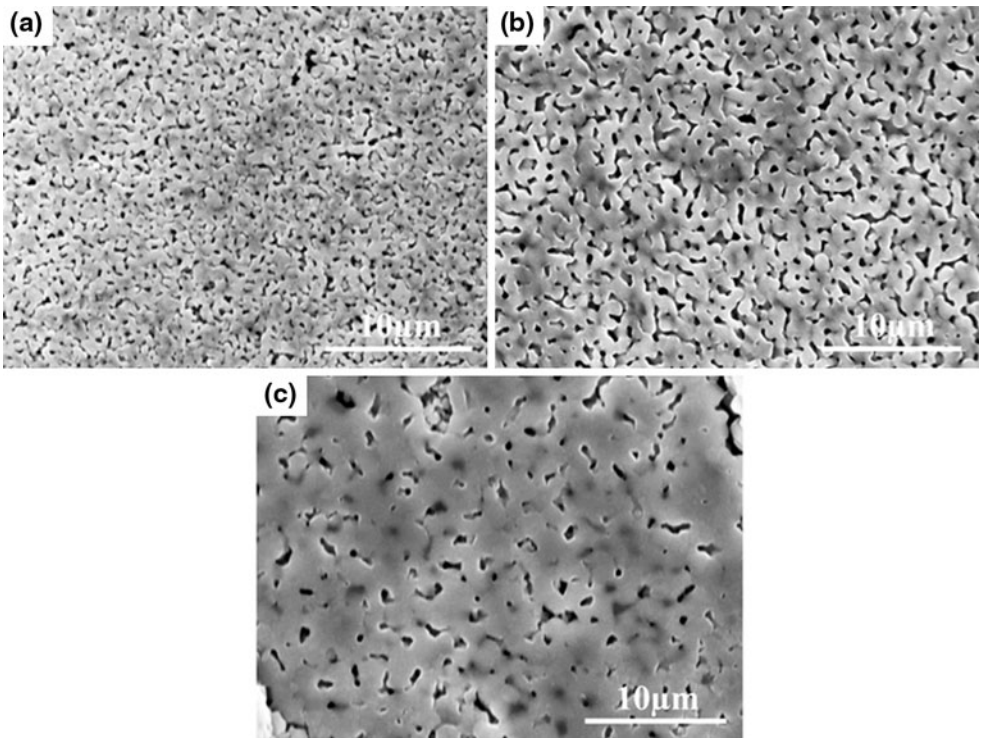

Fig. 2 The SEM micrograph on the surfaces of the 0.35 mol% Nb^{5+}-doped samples sintered at different sintering temperatures; **a** 1,100 °C, **b** 1,160 °C, **c** 1,220 °C

reflections (200) and (002) can not be split into two peaks; however, the ceramics sintered at 1,220 °C show a tetragonal structure in which the reflections (200) and (002) can be split into two peaks. It is indicated that the phase structures of the ceramics obtained at various sintering temperatures may be affected by the crystallite sizes of the ceramics.

3.2 Microstructure of the ceramics

The microstructure of the samples with doped Nb_2O_5 of 0.175 mol% is significantly affected by the sintering temperature (Fig. 2), and the average grain sizes of the samples shown in Fig. 2a–c are 0.63, 0.97 and 1.88 μm, respectively. It can be seen that the grain size of the samples increases with the increasing of the sintering temperature; moreover, the porosities of the ceramics sintered at low temperature are larger than those at high temperature.

3.3 Influence of Nb–dopant on electrical properties

The dependence of the RT resistance of the multilayer BTN ceramics, reoxidized at 600 °C for 1 h after fired at 1,160 °C for 2 h in a reducing atmosphere, on the dopant content is shown in Fig. 3, and the influence of the dopant concentration on the PTCR characteristics is

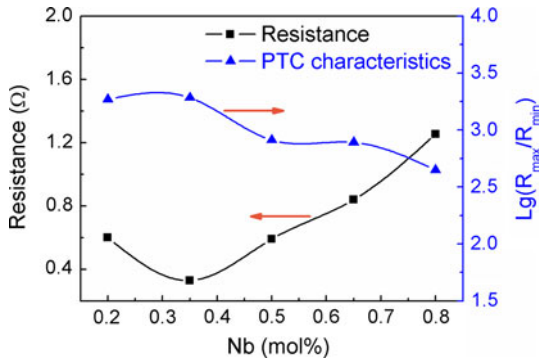

Fig. 3 The room-temperature resistance and the resistance jump as a function of the dopant concentration in the range from 0.2 to 0.8 mol% Nb^{5+}

shown in Fig. 4. From the figures, the RT resistance of the samples first decreases and then increases as a function of the dopant concentration. However, a resistance jump exhibits a contrary tendency. This phenomenon signifies that the most suitable donor–doped content is 0.35 mol% Nb^{5+}, because the smaller the RT resistance is, the higher a resistance jump. Furthermore, the decrease in resistance is generally attributed not only to the electronic compensation of the substituted Ti^{4+} by the Nb^{5+} [14, 19], but also to the formation of the following oxygen vacancies:

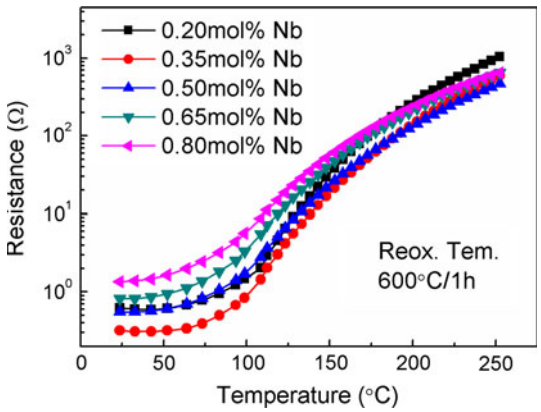

Fig. 4 The temperature dependence of resistance of the samples reoxidized at 600 °C for 1 h after sintering at 1,160 °C for 2 h and for the various doping concentrations

$$2BaO + Nb_2O_5 \rightarrow 2Ba_{Ba} + 2Nb_{Ti}^{\cdot} + 6O_O + {}^1/_2O_2 + 2e' \quad (1)$$

$$O_O \rightarrow V_O^{\cdot\cdot} + {}^1/_2O_2 + 2e' \quad (2)$$

On the other hand, the increase in resistance is mainly due to the ionic compensation resulting from the formation of titanium vacancies [14–16, 18].

$$5BaO + 2Nb_2O_5 \rightarrow 5Ba_{Ba} + 4Nb_{Ti}^{\cdot} + V_{Ti}^{''''} + 15O_O \quad (3)$$

Recently, the available experimental results [20, 21] have been reported the formation of titanium vacancies with high dopant concentrations, and the vacancies as charge compensation defects are preferred over barium vacancies; moreover, the concentration of the titanium vacancies plays a dominant role. Thus, the RT resistance of the samples increases with the increasing of the dopant concentration.

The complex-plane impedance diagrams of the samples in Fig. 3 are exhibited in Fig. 5. Both grain resistance (R_g) and grain-boundary resistance (R_{gb}) can be calculated from

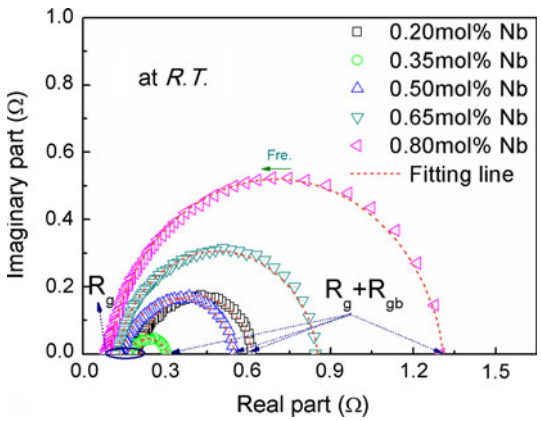

Fig. 5 The complex-plane impedance diagrams of the samples with different dopant concentration

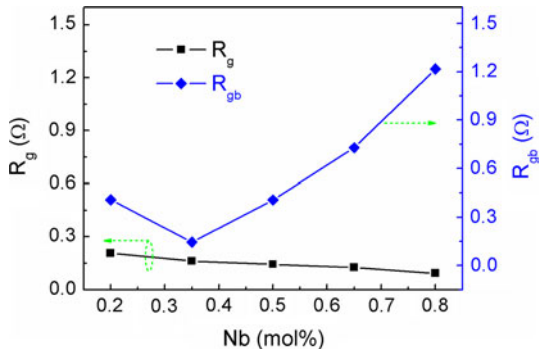

Fig. 6 The room-temperature resistance of the samples with the grains and grain boundaries versus the dopant concentration

Fig. 5 by the least squares method fitting. The results in Fig. 6 indicate that the R_g of the specimens is almost unaffected by the dopant concentration; however, the R_{gb} firstly reduces and then increases versus the dopant concentration and is the lowest at the dopant concentration of 0.35 mol% Nb^{5+}. This is because the RT resistance of the ceramics is considered to be mainly related to that of the grain boundary. Furthermore, the PTCR characteristics are mainly determined by the height of the Schottky barrier of the grain boundary. In addition, it is expected that a small quantity of Ti sites of the ceramics may be substituted by the nickel ions; it is beneficial to improve the height of the Schottky barriers. Thus, we can draw a conclusion that the grain-boundary resistance is affected by the dopant concentration.

3.4 Influence of the sintering temperature on PTCR characteristics

The RT resistance of the multilayer BTN ceramics that are reoxidized at 750 °C for 1 h after firing at different temperatures (1,070–1,220 °C) for 2 h is shown in Fig. 7 as a function of the content of Nb^{5+}, and the influence of the

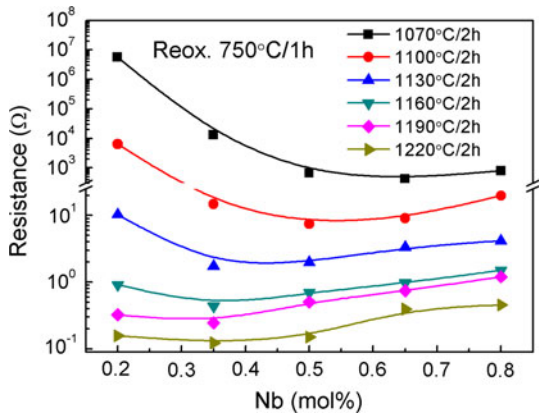

Fig. 7 The room-temperature resistance as a function of the donor-doped concentration at different sintering temperature

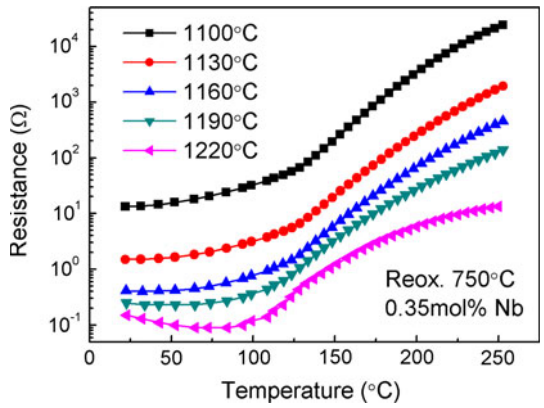

Fig. 8 The temperature dependence of resistance for the BTN ceramics with 0.175 mol% Nb_2O_5 at different sintered temperature

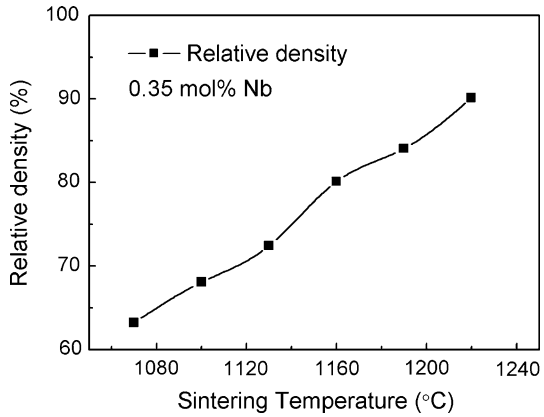

Fig. 9 The relative densities of the ceramics as a function of the sintering temperature

sintering temperature on the PTCR effect is shown in Fig. 8. From the Fig. 7, we can see that the RT resistance of the ceramics first decreases and then increases with an increase in the dopant concentration from 0.2 to 0.8 mol% Nb^{5+} at all sintering temperatures; moreover, it is also found that the corresponding dopant concentration of the minimum resistivity is shifted to lower value with the increasing of sintering temperature; moreover, the moving rate of the dopant concentration is decreased by degrees from 1,070 to 1,160 °C and then keeps at the same level for 1,160–1,220 °C. This phenomenon signifies that the higher the sintering temperature is, the lower the critical dopant concentration. This is because the relative densities of the ceramics obtained at different sintering temperatures are distinct. Figure 9 shows that the relative density of the multilayer BTN ceramics doped with Nb^{5+} of 0.35 mol% at the different sintering temperature of 1,070–1,220 °C. In general, the relative density of the ceramics increases with an increase in the sintering temperature because of an increase of the grain size and decreasing of the porosity, and these results have been confirmed by the data from the Fig. 2. From the Fig. 9, the specimens obtained under a sintering temperature of 1,070 °C have much lower densities than those obtained at 1,220 °C. According to Kuwabara [22], the jump ratio of the ceramics decreases with an increase in their densities due to the porosity of the ceramics. Thus, higher densities of the specimens may deteriorate the PTCR effect because absorption of oxygen during annealing in air becomes difficult.

On the other hand, a low-melting interfacial liquid (Ni, Ba, Ti) layer between $BaTiO_3$ and the Ni electrodes [23] may be formed at temperatures from 1,000 to 1,100 °C, and Yang et al. [24] also reported the existence of the interfacial layer, whose thickness [25] is about 5–10 nm between Ni and $BaTiO_3$, thus the interfacial layer of the BTN ceramics obtained at a low sintering temperature of 1,070–1,100 °C may be easily formed. Furthermore, a certain extent of Ni diffusion to the BTN ceramics near the interfacial layer is favorable to enhance the PTCR characteristics of the samples, because NiO may be distributed in the $BaTiO_3$ films on Ni foil [25] after annealing in air. Therefore, the low sintering temperature is helpful to improve the resistance jump of the samples, and increase the RT resistance.

Figure 10 shows the EDS analysis of the multilayer BTN ceramics with doped Nb_2O_5 of 1.75 mol% fired at the sintering temperature of 1,100 °C. The results indicate that the rate of Ba:Ti:Ni:O of spot A (near the Ni electrodes) is approximately 1:1:1:5.1, which is about consistent with the composition of $BaTiO_3$–NiO. This suggests that the EDS data of the spot A confirmed the Ni ion have been oxidized near Ni internal electrodes, thus the RT resistance of the samples obtained at low sintering temperature will be increased. The rate of Ba:Ti:O of spot B (in the middle of dielectric layer) is approximately 1:1.1:4, which is also about consistent with the composition of $BaTiO_3$–Nb_2O_5. It is indicated that the Ti^{4+} iron (B sites) has been substituted by the Nb^{5+} iron in the BTN matrix (a perovskite structure; ABO_3).

3.5 Influence of the sintering time on PTCR effect

Figure 11 shows that both the RT resistance and its resistance-jump ratio ($Lg(R_{max}/R_{min})$) of the multilayer BTN samples doped with 0.35 mol% Nb^{5+} which is reoxidized at 600 °C for 1 h after sintering at 1,160 °C for the different sintering time of 0.5–6 h, and the temperature dependence of resistance for the samples is shown in Fig. 12. Obviously, both the RT resistance and the jump ratio of the samples decrease with the increasing of sintering time across the range of 0.5–6 h. The highest resistance-jump ratio is obtained at the sintering time of 0.5 h, which is larger by 3.4 orders of magnitude, with the RT resistance being 1.26 Ω. However, the lowest resistance

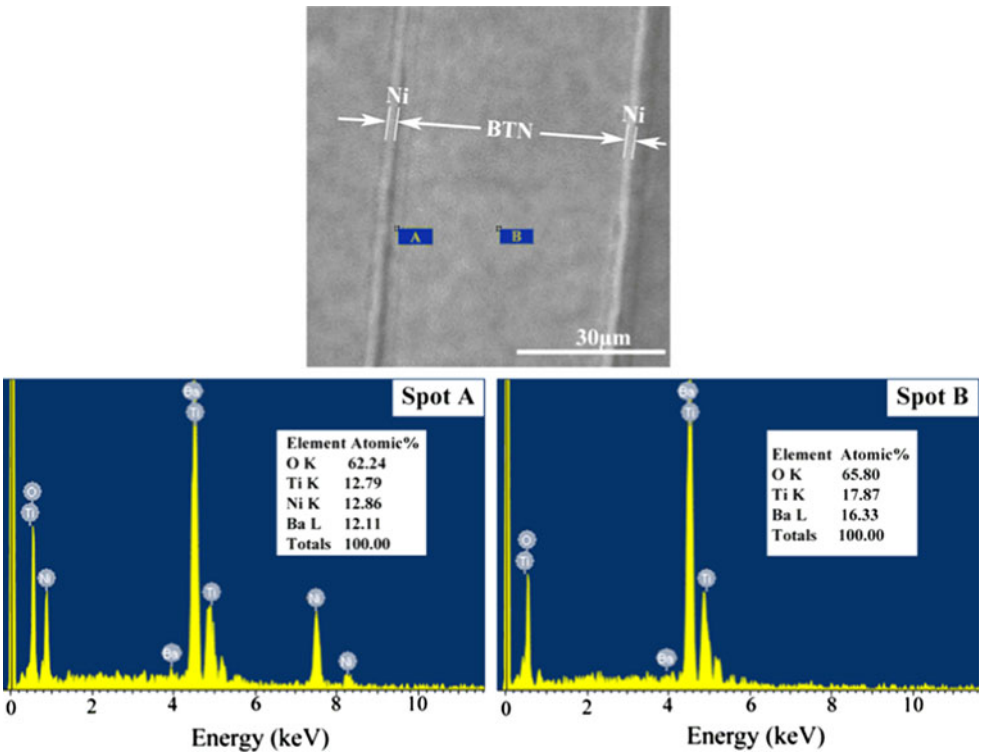

Fig. 10 EDS analysis of the BTN samples with 0.175 mol% of Nb_2O_5 sintered at 1,100 °C for 2 h

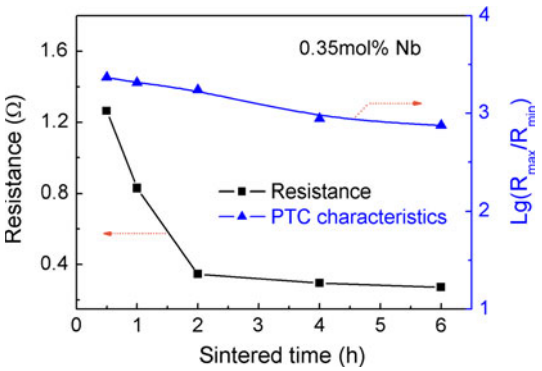

Fig. 11 The room-temperature resistance and the resistance jump of the BTN ceramics as a function of the sintering time

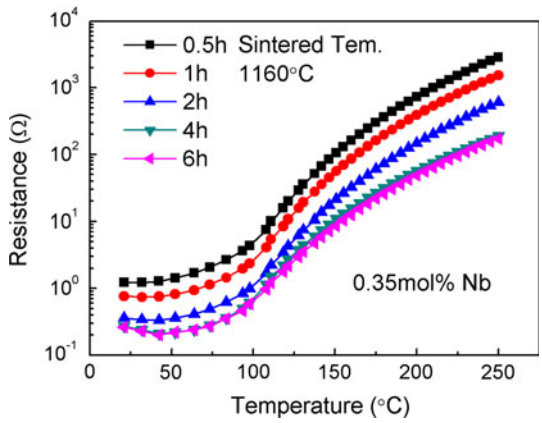

Fig. 12 The temperature dependence of resistance of the BTN samples doped with 0.175 mol% Nb_2O_5 at different sintering time of 0.5–6 h

jump is obtained at the sintering time of 6 h, which is slightly larger by 2.9 orders of magnitude, with the RT resistance being 0.27 Ω. The results show that BTN ceramics obtained at a lower sintering time have modest RT resistance and PTCR effect, which indicates that the concentration of the oxygen vacancies and electrons increases with an increase in the sintering time from the Eq. 2. In addition, the grain sizes of the ceramics may increase with the increasing of the sintering time of 0.5–6 h, and the porosity of the ceramics obtained at long sintering time can be reduced. Consequently, it is found that the diffusion and permeation of oxygen atoms from the air into compact ceramics become difficult during annealing treatment. According to the following expression $V_O^{\cdot\cdot} + {}^1/_2O_2 + 2e' \rightarrow O_O$, the localized electrons and oxygen vacancies around the defects are incompletely annihilated; therefore, the RT resistance of the ceramics obtained at a long sintering time is reduced.

3.6 Acceptor-state density (N_s)

According to the Heywang–Jonker model [3–5], when the temperature of the sample is above the T_C, the height of the potential barrier (ϕ) is given by the expression

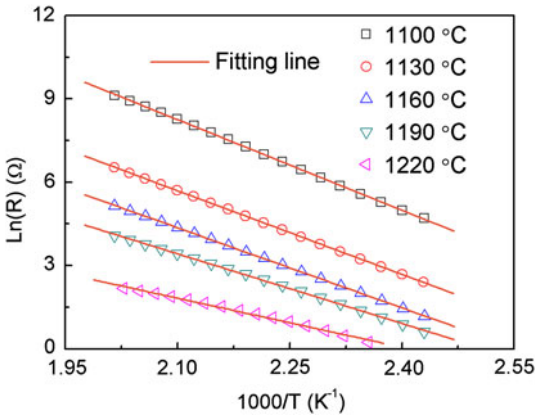

Fig. 13 Arrhenius plots of lnR against 10^3/T for the 0.35 mol% Nb-doped ceramics obtained at different sintering temperature of 1,100–1,220 °C

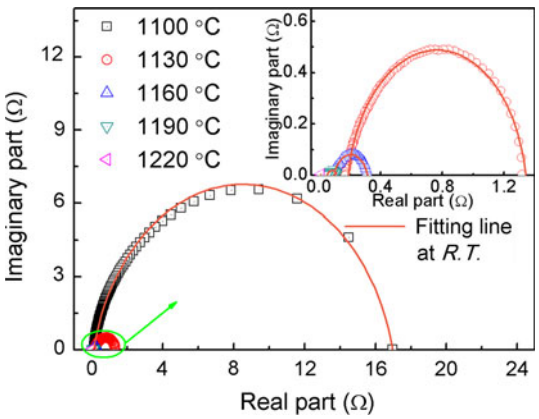

Fig. 14 The complex-plane impedance diagrams of the samples with different sintering temperature

$$\phi = eN_S^2/8\varepsilon_0\varepsilon_r N_d \tag{4}$$

and the temperature dependence of the relative permittivity is described by the Curie–Weiss law:

$$\varepsilon_r = C/(T-\theta) \tag{5}$$

where N_s is the acceptor-state density, e is the electric charge, ε_0 is the permittivity in free space, ε_r is the relative permittivity of the $BaTiO_3$ ceramics, N_d is the donor concentration, C is the Curie constant ($\sim 1.5 \times 10^5$ K) [26–29], T is the absolute temperature, and θ is the Curie–Weiss temperature ($\theta = 383$ K) [1, 2]. Heywang found that the resistivity is given by the following formula:

$$\rho = \alpha\rho_0 \exp(e\phi/kT) \tag{6}$$

where k is the Boltzmann constant and ρ_0 is a constant. Therefore, the slope (λ) of the Arrhenius plot lnρ versus T^{-1} is introduced, and the slope can be calculated from Eqs. 4–6 with the following formula:

$$\lambda = -e^2\theta N_s^2/8k\varepsilon_0 C N_d \tag{7}$$

where N_d is given by the following formula: $N_d = 1/e\mu\rho_g$, where the ρ_g can be obtained by the complex impedance analysis, μ is the electron mobility of $BaTiO_3$ ($\mu = 0.5$ cm^2 V^{-1} s^{-1}) [29]. Figure 13 shows that Arrhenius plots of ln$R$ against $10^3/T$ for the 0.35 mol% Nb^{5+}-doped $BaTiO_3$ ceramics obtained at different sintering temperature of 1,100–1,220 °C. The complex-plane impedance diagrams of the samples in Fig. 13 are shown as in Fig. 14. The resistance of the grain boundary is estimated from Fig. 14, the results show that the grain-boundary resistance decrease with the increasing sintering temperature of 1,130–1,220 °C; moreover, the PTCR effect of the samples obtained at low sintering temperature is improved because the reoxidation of their grain boundary is more easy than that of the samples sintered at high sintering temperature. In addition, the value of the acceptor-state density, as calculated from Eq. 7 for the samples sintered at the different sintering temperatures of 1,130–1,220 °C for 2 h, is in the range from 2.47×10^{13} to 7.19×10^{13} cm^{-2}, as shown in Table 1, a higher sintering temperature leads to higher acceptor-state density, which indicates an increase in the amount of oxygen atoms absorbed at the grain boundaries [5]. Meanwhile, the thickness of the depletion layer (b; $b = N_s / 2N_d$) decreases with the increasing sintering temperature of 1,130–1,220 °C as shown in Table 1, therefore, the PTCR characteristics of the samples obtained at a high sintering temperature of 1,220 °C are deteriorated. However, the b increases with the increasing sintering temperature in the range from 1,100 to 1,130 °C, this is because that the grain resistance of the sample sintered at 1,100 °C is lower than those at 1,130 °C in Table 1 using the following formula: $b = e\mu N_s\rho_g / 2$.

Table 1 The grain-boundary resistivity, the donor concentration N_d, the acceptor-state density N_s and the thickness of the depletion layer b of BTN ceramics sintered at different temperatures for 2 h

Firing temperature/°C	Samples				
	$\lvert\lambda\rvert/10^3$ K^{-1}	ρ_g/Ω·cm	$N_d/10^{18}$ cm^{-3}	$N_s/10^{13}$ cm^{-2}	b/nm
1,100	10.87	25.7	0.49	2.81	288.8
1,130	10.04	30.8	0.41	2.47	304.3
1,160	9.61	14.4	0.87	3.54	203.1
1,190	8.35	9.0	1.39	4.16	149.9
1,220	5.89	2.1	5.87	7.19	61.2

4 Conclusions

The influence of the sintering conduction on the PTCR characteristics of the mutilayer BTN-based ceramics with Ni internal electrode sintered at 1,070–1,220 °C for 2 h in a reducing atmosphere and reoxidized at 600 °C for 1 h in air has been investigated. The results show that the RT resistance or the grain-boundary resistance of the ceramics first reduces and then increases as a function of the donor–doped concentration, and the critical concentration of the dopant closely depends on the sintering temperature. Moreover, we found that both the RT resistance and the PTCR effect of the ceramics decrease with an increase in the sintering temperature or the sintering time. The BTN ceramics obtained at a low reoxidized temperature of 600 °C after sintering at 1,160 °C showed a remarkable PTCR effect, with a resistance jump larger by 3.3 orders of magnitude, along with a low RT resistance of 0.3 Ω. Furthermore, the acceptor-state density of the samples sintered at the sintering temperature of 1,130–1,220 °C is in the range from 2.47×10^{13} to 7.19×10^{13} cm^{-2}.

Acknowledgments This work was financially supported by the Ministry of Science and Technology of China through 863 Program (no. 2009AA03Z445).

References

1. M.W. Mancini, P.I. Paulin Filho, J. Appl. Phys. **100**, 104501 (2006)
2. J. Illingsworth, H.M. Ai-Allak, A.W. Brinkman, J. Woods, J. Appl. Phys. **67**, 2088–2092 (1990)
3. W. Heywang, J. Am. Ceram. Soc. **47**, 484 (1964)
4. W. Heywang, Solid State Electron. **3**, 51 (1961)
5. G.H. Jonker, Solid State Electron. **7**, 895–903 (1964)
6. P.H. Xiang, H. Harinaka, H. Takeda, T. Nishida, K. Uchiyama, T. Shiosaki, J. Appl. Phys. **104**, 094108 (2008)
7. W.H. Yang, Y.P. Pu, X.L. Chen, J.F. Wang, J. Phys.: Conference Series **152**, 012040 (2009)
8. Z.C. Lia, H. Zhang, X.D. Zou, Mater. Sci. Eng. **B 116**, 35 (2005)
9. A. Kanda, S. Tashiro, H. Igarashi, Jpn. J. Appl. Phys. **33**, 5431–5434 (1994)
10. H. Niimi, K. Mihara, Y. Sakabe, M. Kuwabara, Jpn. J. Appl. Phys. **46**(10A), 6715–6718 (2007)
11. H. Niimi, Hikone, A. Ando, Omihachiman, U.S. Patent 7,348,873 B2 (2008)
12. Y.K. Chung, S.C. Choi, J. Korean Chem. Soc. **46**, 330–335 (2009)
13. G.H. Jonker, E.E. Havinga, Mat. Res. Bull. **17**, 345 (1982)
14. H.M. Chan, M.P. Harmer, D.M. Smyth, J. Am. Ceram. Soc. **69**(6), 507 (1986)
15. E. Brzozowski, M.S. Castro, J. Eur. Ceram. Soc. **24**, 2499–2507 (2004)
16. E. Brzozowski, M.S. Castro, C.R. Foschini, B. Stojanovic, Ceram. Int. **28**, 773–777 (2002)
17. E. Brzozowski, M.S. Castro, J. Mater. Process. Technol. **168**, 464–470 (2005)
18. J. Nowotny, M. Rekas, Defect Struct. Ceram. Int. **20**, 265–275 (1994)
19. Y.P. Pu, H.D. Wu, J.F. Wei, B. Wang, J. Mater. Sci.: Mater. Electron. **22**, 1480 (2011)
20. M.T. Buscaglia, V. Buscaglia, M. Viviani, P. Nanni, M. Hanuskova, J. Eur. Ceram. Soc. **20**, 2004 (2000)
21. F.D. Morrison, D.C. Sinclair, A.R. West, J. Am. Ceram. Soc. **84**, 474–476 (2001)
22. M. Kuwabara, J. Am. Ceram. Soc. **64**, 639–644 (1981)
23. A.V. Polotai, G.Y. Yang, E.C. Dickey, C.A. Randall, J. Am. Ceram. Soc. **90**, 3811 (2007)
24. G.Y. Yang, S.I. Lee, Z.J. Liu, C.J. Anthony, E.C. Dickey, Z.K. Liu, C.A. Randall, Acta Mater. **54**, 3515 (2006)
25. T. Dechakupt, G. Yang, C.A. Randall, S. Trolier-McKinstryw, J. Am. Ceram. Soc. **91**, 1845–1850 (2008)
26. H.P. Chen, T.Y. Tseng, J. Mater. Sci. Lett. **8**, 1483–1485 (1989)
27. Y.H. Hu, M.P. Harmer, D.M. Smyth, J. Am. Ceram. Soc. **68**, 372 (1985)
28. C.J. Johnson, Appl. Phys. Lett. **7**, 221 (1965)
29. B. Huybrechts, K. Ishízaki, M. Takata, J. Am. Ceram. Soc. **75**, 722–724 (1992)